



# **Seasonal Interplay of Water Mass Mixing and Nutrient Dynamics**

in an Arctic Fjord: A Case Study of Kongsfjorden, Svalbard

3	
4	Hyebin Kim <sup>1</sup> , Dukki Han <sup>2</sup> , Sang Rul Park <sup>3</sup> , Tae-Hoon Kim <sup>1*</sup>
5	
6	<sup>1</sup> Department of Oceanography, Faculty of Earth Systems and Environmental Sciences, Chonnam National
7	University, Gwangju 61186, Republic of Korea
8	<sup>2</sup> Department of Marine Molecular Bioscience, Gangneung-Wonju National University, Gangneung 25457,
9	Republic of Korea
10	<sup>3</sup> Department of Marine Life Sciences, Jeju National University, Jeju 63243, Republic of Korea
11	
12	
13	*Corresponding author:
14	E-mail. Address: thkim80@jnu.ac.kr. (TH. Kim)
15	
16	
17	
18	





### Abstract

19

20

21

22

23

24

25

26

27

28

29

30

31

32

33

34

35

36

37

38

39

40

41

This study examined seasonal variations in water mass structure and nutrient dynamics in Kongsfjorden, a high Arctic fjord where water mass composition varies seasonally due to mixing among Atlantic Water, Polar Surface Water, and glacial meltwater. In spring, the dominance of Modified Atlantic Water (MAW) facilitated active vertical mixing, leading to relatively high, uniform nutrient concentrations throughout the water column. In summer, the enhanced influence of glacial meltwater and warmer Polar Surface Waters (PSWw) resulted in strong surface stratification and significant nutrient depletion in the upper layer. To disentangle the effects of physical mixing from biological consumption, theoretical nutrient concentrations were calculated based on a four-component water mass mixing model. The positive differences between theoretical and observed concentrations (\Delta Nutrient) were indicative of significant biological uptake, which accounted for substantial nutrient reductions in observed surface concentrations from spring to summer: approximately  $69 \pm 18\%$  for nitrate,  $74 \pm 15\%$  for phosphate, and  $47 \pm 18\%$  for silicate. Crucially,  $\Delta$ Nutrient values served as a 'biogeochemical memory,' reflecting the cumulative net biological consumption since the spring bloom rather than just instantaneous phytoplankton biomass. These biological processes also altered nutrient stoichiometry, causing the surface nitrogen-to-phosphorus (N/P) ratio to increase from 15.0 in spring to 18.8 in summer, indicating a shift in nutrient limitation patterns. Consequently, summer surface waters transitioned toward potential co-limitation, with concentrations of phosphate ( $\sim 0.13 \pm 0.07 \, \mu\text{M}$ ) and silicate ( $\sim 1.66 \pm 0.39 \, \mu\text{M}$ ) approaching their respective limitation thresholds. These findings highlight a clear seasonal transition from a physically controlled, nutrient-replete spring to a biologically regulated, nutrient-limited summer. This understanding is crucial for predicting how Arctic fjord ecosystems, and their primary





- 42 productivity, will respond to ongoing Atlantification and increased freshwater input under
- 43 climate change.

58

59

60

61

62

63

#### 1. Introduction

45 The Arctic marine ecosystem, which is characterized by unique and dynamic environmental conditions, is governed by the complex interaction of physical, chemical, and biological factors. 46 47 Within this system, nutrient availability, which is primarily controlled by ocean currents, riverine discharge, and atmospheric deposition, plays a fundamental role in maintaining 48 49 biological productivity and ecological health (Duarte et al., 2012; Tovar-Sánchez et al., 2010). 50 These nutrients are particularly vital for primary production, which is the foundation of the Arctic marine food web. Ocean currents, notably Atlantic and Pacific inflows, transport 51 52 essential nutrients into the Arctic Ocean, thus influencing regional primary productivity 53 (Carmack et al., 2006; Codispoti et al., 2013; Torres-Valdés et al., 2013). As a result, seasonal fluctuations in sea ice, solar radiation, and water column stratification drive nutrient dynamics 54 and productivity cycles (Arrigo et al., 2017). In particular, during spring and summer, increased 55 sunlight and meltwater often promote stratification and phytoplankton blooms (Leu et al., 2015; 56 57 Tremblay et al., 2015).

Arctic fjords such as Kongsfjorden in Svalbard are useful areas for assessing nutrient cycling processes due to the interactions between advected ocean currents (e.g., warm, saline Atlantic Water) and local water masses (Cottier et al., 2005; Svendsen et al., 2002). The inflow of nutrient-rich Atlantic Water can significantly affect the nutrient supply and productivity in fjords, leading to complex spatiotemporal variability (Carmack et al., 2006). Understanding these dynamics, especially before and after blooms, is therefore essential for predicting how





81

82

83

84

85

86

64 Arctic fjord ecosystems respond to environmental changes. This is because seasonal shifts in 65 nutrient availability and plankton community structure strongly influence the region's 66 fundamental biogeochemical processes (Tremblay et al., 2015; Vonnahme et al., 2022; Singh 67 et al., 2020). Water mass mixing significantly influences nutrient distribution in Arctic fjords 68 (Randelhoff et al., 2018; Hodal et al., 2012; Tamelander et al., 2013; Rysgaard et al., 1999). 69 While AW inflow can enhance productivity by supplying nutrients (Carmack et al., 2006; 70 Torres-Valdés et al., 2013), a quantitative understanding of how physical mixing and biological 71 processes separately contribute to seasonal nutrient depletion remains a key knowledge gap. 72 Disentangling these effects is critical for accurately assessing the biological drivers of 73 productivity. 74 The present study addresses these gaps by examining seasonal (spring/summer) variation in 75 water mass mixing and nutrient dynamics in Kongsfjorden. Specifically, we employ a nutrient anomaly approach (\Delta Nutrient) derived from a water mass mixing model to quantify the net 76 biological impact on the nutrient inventory. Furthermore, we intend to determine the impact of 77 78 these seasonal mixing patterns, notably the active vertical mixing characteristic of spring and 79

biological impact on the nutrient inventory. Furthermore, we intend to determine the impact of these seasonal mixing patterns, notably the active vertical mixing characteristic of spring and the enhanced stratification observed in summer on nutrient concentrations. A key aspect of our research will be to explore whether differences between theoretical nutrient concentrations, derived from mixing models, and actual observed nutrient levels can be effectively used to discern the influence of biological processes. Specifically, this study tests the hypothesis that the difference between theoretical (mixing-derived) and observed nutrient concentrations can effectively quantify the cumulative influence of biological processes. By comparing these observed and theoretical nutrient levels, this study will assess the relative influence of physical mixing versus biological processes. Ultimately, this research aims to provide crucial baseline





- 87 data for understanding how Arctic marine ecosystems respond to climate change, particularly
- 88 in the context of warming-induced alterations to water masses and mixing dynamics within
- 89 sensitive fjord environments.

## 2. Materials and Methods

## 2.1 Study Sites

90

91

99

104

- 92 Kongsfjorden, an Arctic fjord situated on the west coast of Spitsbergen, Svalbard, was used
- 93 as the primary study site (Fig. 1). This fjord is approximately 20 km in length and varies in
- 94 width from 4 to 10 km, reaching a maximum depth of approximately 300 m near its mouth.
- 95 The hydrography in Kongsfjorden is characterized by significant freshwater input from several
- 96 tidewater glaciers, a process that is more intense during the summer melt season. Furthermore,
- 97 the fjord is influenced by the advection of relatively warm and saline AW transported via the
- 98 West Spitsbergen Current and by the presence of colder, fresher waters of Arctic origin.

#### 2.2. Sampling and Analytical Methods

Seawater samples were collected from three discrete depths within vertical water columns using a conductivity-temperature-depth (CTD) rosette system aboard the MS Teisten (April)

102 and the RV Helmer Hanssen (July) during 2023 in Svalbard. Sampling depths were adjusted

by season to capture key hydrographic features. In spring (April), samples were collected at 0

m (surface), 20 m (mid-depth), and 50 m (deep) to represent the well-mixed water column. In

105 summer (July), a more stratified sampling strategy was employed to resolve the sharp vertical

gradients caused by meltwater; samples were collected from 0–5 m (surface), 10–25 m (mid-





depth, capturing the thermocline), and 50–100 m (deep). Detailed station-specific depths are provided in the caption of Figure 4. During sample collection, the salinity and temperature were measured using sensors within the CTD system. Fluorescence was measured using a CTD-attached fluorometer and is presented in fluorescence-derived chlorophyll-*a* concentrations (mg/m³).

Dissolved inorganic nutrients (NO²-, NO³-, PO₄³-, and Si(OH)₄) were analyzed using a nutrient autoanalyzer (New QuAAtro39; SEAL Analytical, UK). For each nutrient, 50 mL of seawater was filtered through 0.7 μm GF/F filters (25 mm, Whatman Inc., Florham Park, NJ, USA). This filtration was conducted using acid-washed syringes, and the filtrate was collected in polypropylene conical tubes, which were stored at −20°C until analysis. To ensure the accuracy and precision of the nutrient analysis, certified reference materials for each nutrient were run concurrently with the samples. According to the certified reference material (KANSO Co., LTD), the analytical uncertainty was within 5% for nitrate (the sum of NO₂- and NO₃-), Si(OH)₄, and PO₄³-. Hereafter, the sum of nitrate (NO₃-) and nitrite (NO₂-) is referred to as NOx, PO₄³- as phosphate, and Si(OH)₄ as silicate. This terminology is used to ensure accuracy as

## 2.3. Water Mass Analysis and Theoretical Nutrient Concentrations

nitrite concentrations, while minor, were not consistently negligible..

To assess the seasonal variability in the hydrographic structure of the fjord and its influence on the distribution of nutrients, water mass analysis was conducted. The mixing ratios of the different water masses present in Kongsfjorden were calculated using observed temperature and salinity data for both spring and summer. This analytical approach was in accordance with





129

130

131

132

133

134

135

136

137

138

139

140

141

142

143

144

145

146

147

148

149

established methodologies detailed by Miller (1950) and Tomczak (1999), which require the precise definition of characteristic end-member water types that contribute to the observed water properties within the fjord. Nutrient concentrations for the end-members were adopted from the comprehensive study of Duarte et al. (2021), which provides representative background values for the water masses advected into the Svalbard region.

In the present study, four principal end-member water types were used in the mixing model due to their characteristic presence and influence in the Arctic region and specifically in Kongsfjorden: Atlantic Water (AW), Modified AW (MAW), Polar Surface Water (PSW), and its warmer variant Polar Surface Water warm (PSWw). While glacial meltwater (GMW) is a significant source of freshwater in summer, its direct influence was simplified and incorporated into the characteristics of PSWw, which represents the warm, low-salinity surface layer. This assumption is further addressed in the discussion regarding silicate dynamics. The selection of these water types was consistent with previous hydrographic characterization of the region (Nilsen et al., 2008; Rudels et al., 2000). AW, which is defined by its relatively high temperature and salinity, originates from lower latitudes and is advected into the Arctic. MAW represents AW that has undergone significant transformation through cooling, freshening, and nutrient alteration following its entry and circulation within the Arctic system. PSW is characterized by its cold temperatures and lower salinity, typically occupying the upper layers of the water column and originating from Arctic surface processes. PSWw shares many of the same general characteristics as PSW but is distinguished by notably warmer temperatures, often reflecting the influence of seasonal surface heating and increased meltwater input, particularly during the summer months.



151

152

153

154

155

156

157

158

159

160

161

162

163

164

165

166

167

168

169

170



The temperature-salinity (T-S) characteristics defining these end-members are detailed in Table 1 and visually represented in Fig. 2a. These definitions were carefully established based on a combination of established values from past research (e.g., Rudels et al., 2000) and an examination of the observed distribution of T-S data collected during the present study. This dual approach ensured that the defined end-members comprehensively and accurately covered the full spectrum of water types observed in Kongsfjorden during the sampling periods. Because the hydrographic properties of the deep-water masses in Kongsfjorden exhibited minimal temporal variation between the spring and summer seasons, a single, consistent set of T-S characteristics for each end-member was employed for water mass analysis in both the spring and summer datasets, allowing for a direct comparison of seasonal shifts in their relative contributions.

The fractional contribution of AW, MAW, PSW, and PSWw (denoted as A, B, C, and D, respectively, Table. 1) to any given water sample (P) collected within the fjord was calculated using a standard four end-member mixing model (Fig. 2b). This model operates on the principle of the conservative mixing of temperature and salinity (Miller, 1950). The output of this model provides the fractional contributions  $(f_A, f_B, f_C, \text{ and } f_D)$  of each end-member to the sampled water under the fundamental constraint that the sum of these individual fractions equals unity (i.e.,  $f_A + f_B + f_C + f_D = 1$ , or 100%).

Theoretical nutrient concentrations (Nutrient\*) for each sample were calculated by multiplying the fraction of each end-member water mass (defined in Table 1) by its endmember nutrient concentration  $(Nut_x)$  and summing the contributions as follows:

Nutient\* = 
$$(f_A \times Nut_A) + (f_B \times Nut_B) + (f_C \times Nut_C) + (f_D \times Nut_D)$$





- To assess the biological impact on nutrient concentrations, the difference (ΔNutrient)
- between the theoretical and observed concentrations was calculated:
- 174  $\Delta Nutrient = Nutrient^* Nutrient_{observed}$
- 175 A positive value indicated net nutrient removal beyond physical mixing, which was attributed
- to the net biological effect, primarily biological consumption.
- To evaluate the robustness of these calculations, we performed a sensitivity analysis to 177 quantify the uncertainty propagated from the end-member nutrient definitions. The end-178 member concentrations for NOx, phosphate, and silicate were varied by  $\pm 10\%$ , a range selected 179 as a conservative estimate of natural variability based on regional oceanographic studies (e.g., 180 181 Torres-Valdés et al., 2013; Hopwood et al., 2020). The resulting range in the calculated ΔNutrient values was used to define the uncertainty of our model-derived results, which is 182 183 reported alongside our key quantitative findings. This assessment provides a measure of 184 confidence in our conclusions against potential variations in the end-member characteristics.

## 2.4. Statistical analysis

- All statistical analyses were performed using SPSS ver. 19 (IBM Corp., Armonk, NY, USA).
- 187 Prior to hypothesis testing, the normality of the data was assessed using the Shapiro-Wilk test.
- 188 Depending on the results of the normality test, either independent samples t-tests (for normally
- distributed variables) or Mann-Whitney U tests (for non-normally distributed variables) were
- applied to compare differences between groups. A significance level of p < 0.05 was used for
- 191 all tests.





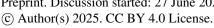
## 3. Results and Discussion

## 3.1. Seasonal Variation in Hydrography and Observed Dissolved Inorganic Nutrient

#### **Levels**

Kongsfjorden exhibited distinct seasonal hydrographic conditions during the study period (Fig. 3). Water temperatures in the fjord ranged from a minimum of -0.86°C to a maximum of 6.88°C (Fig. 3a), and salinity ranged from a minimum of 28.05 to a maximum of 34.93 (Fig. 3b). The spring season was characterized by lower temperatures, with a mean temperature of  $0.16 \pm 0.56$ °C, and relatively high and uniform salinity, averaging  $35.67 \pm 0.28$ . In contrast, summer had significantly warmer waters (mean:  $3.56 \pm 1.49$ °C) and markedly lower and more variable salinity (mean:  $33.03 \pm 1.92$ ). These hydrographic changes were primarily driven by seasonal increases in solar radiation, sea ice meltwater, and glacial freshwater input, which collectively enhanced the vertical stratification of the water column.

Consistent with these hydrographic shifts, the levels of dissolved inorganic nutrients also exhibited strong seasonal patterns. The NOx concentration varied from 0.67  $\mu$ M to 10.41  $\mu$ M (Fig. 3c). During spring, the mean surface nitrate level was 7.10  $\pm$  1.83  $\mu$ M. In summer, however, mean surface nitrate concentrations decreased significantly to 2.20  $\pm$  1.15  $\mu$ M, representing an approximate 69  $\pm$  18% reduction from spring levels. While surface nitrate was depleted, concentrations in deeper water remained high, resulting in a stronger vertical gradient in summer compared to that in spring. This suggests that active vertical mixing replenished surface nutrients in spring, whereas reduced mixing and significant biological uptake occurred during the summer period.





214

215

216

217

218

219

220

221

222

223

224

225

226

227

228

229

230

231

232

233

234



Phosphate concentrations ranged from 0.07 µM to 0.70 µM (Fig. 3d). The spring surface mean was  $0.50 \pm 0.12 \mu M$ , declining considerably to  $0.13 \pm 0.07 \mu M$  during summer, a reduction of approximately  $74 \pm 15\%$ . Notably, summer phosphate concentrations often fell below the 0.20 µM threshold commonly regarded as limiting for phytoplankton growth in Arctic waters (Tremblay et al., 2015). Thus, there was a strong likelihood of phosphate limitation during this period, particularly given that phosphate declined at a greater rate than nitrate from spring to summer. Silicate concentrations ranged from 0.83 to 4.45 µM (Fig. 3e). The mean surface concentration was  $3.11 \pm 0.72 \, \mu M$  in spring, decreasing to  $1.66 \pm 0.39 \, \mu M$  in summer, representing a  $47 \pm 18\%$  reduction. The summer surface silicate concentration approached the 2 µM threshold frequently cited as indicative of potential silicate limitation for diatom growth (Egge & Aksnes, 1992). In some samples, the summer surface silicate concentrations were higher than expected despite biological uptake, likely due to the influence of glacial meltwater enriched in silicate via bedrock erosion (Hawkings et al., 2017). Statistical analysis confirmed that the seasonal differences observed for all three nutrients were significant (p < 0.05 for all comparisons). These observed nutrient patterns in Kongsfjorden were largely consistent with findings from previous studies in the same location (e.g., Leu et al., 2015). However, the background nutrient levels observed in this study were generally higher than those reported for some other Arctic regions, such as Young Sound, Greenland (Rysgaard et al., 1999), a difference attributable to the stronger and more direct influence of nutrient-rich AW in the Svalbard region. Spatial differences were also apparent within Kongsfjorden; in particular, stations with higher contributions from PSWw exhibited





more pronounced summer surface nutrient depletion, particularly for phosphate, which had mean concentrations as low as  $0.08 \pm 0.03 \,\mu\text{M}$ . (This observation will be further discussed in the context of nutrient limitation in Section 3.4). This likely reflects the influence of glacial meltwater input and enhanced stratification associated with PSWw-dominated surface layers.

#### 3.2. Seasonal Characteristics of Water Masses and Theoretical Nutrient Concentrations

The four-component end-member mixing model revealed distinct seasonal distributions of water masses within Kongsfjorden (Fig. 4). Overall, MAW, with a mean contribution of  $52 \pm 29\%$ , and AW ( $20 \pm 16\%$ ) were the dominant water masses influencing the fjord. These water masses are recognized as the primary sources of inorganic nutrients in this system. The contributions of PSW ( $14 \pm 13\%$ ) and PSWw ( $14 \pm 14\%$ ) were lower on average, though their influence varied considerably with season and depth.

During the spring season, the proportion of MAW was generally higher throughout the water column than in summer, suggesting the active mixing of the inflowing AW and the resident PSW. This mixing is facilitated by physical and chemical processes in the Arctic Ocean that promote the formation of MAW (Rudels et al., 2004), resulting in a relatively uniform vertical distribution of water masses from the surface to the deep layers of the fjord. In contrast, the summer season was characterized by a marked shift in the water mass composition. The surface layer (0-30 m) had a considerably higher proportion of PSWw (33  $\pm$  25%) and PSW (19  $\pm$  16%), which was primarily associated with seasonal sea ice meltwater, surface warming, and freshwater-induced stratification. However, the deep layer (>50 m) remained dominated by AW (36  $\pm$  3%) and MAW (53  $\pm$  3%). This vertical stratification limited the vertical exchange of water and nutrients between the surface and deep layers.





The observed water mass distribution patterns were broadly consistent with previous descriptions of Kongsfjorden by Svendsen et al. (2002) and Cottier et al. (2005). However, the proportion of MAW observed in this study was substantially higher than reported in some earlier studies, which may reflect the ongoing process of Atlantification, which is the enhanced penetration of Atlantic-origin waters into the Arctic Ocean (Polyakov et al., 2017), or be the result of long-term changes in the Arctic hydrography and climate. This trend suggests that future warming could further intensify the influence of warm, saline Atlantic-origin waters, fundamentally altering the fjord's stratification and nutrient supply regimes. Additionally, continued glacier melting driven by regional warming is expected to increase the volume of PSWw, thus intensifying surface stratification in the future.

#### 3.3. Biological Impact on Nutrient Concentrations: Differences between Observed and

# Theoretical Concentrations (\( \Delta \text{Nutrient} \)

To assess the biological influence on nutrient dynamics, the observed nutrient concentrations were compared to theoretical values derived from end-member mixing (Fig. 5). The difference represents net nutrient removal that exceeds a level that can be explained by physical mixing alone. A positive  $\Delta$ Nutrient value indicates that observed concentrations are lower than expected from conservative mixing, thus suggesting biological uptake or transformation. With few exceptions, observed nutrient concentrations were significantly lower than theoretical values (p < 0.05 for all three nutrients), resulting in consistently positive  $\Delta$ Nutrient values. This provides strong evidence for substantial nutrient removal in Kongsfjorden beyond what can be accounted for by physical advection and mixing, with phytoplankton uptake the most likely mechanism.





280

281

282

283

284

285

286

287

288

289

290

291

292

293

294

295

296

297

298

299

300

Seasonal and depth-related comparisons of \( \Delta \)Nutrient values highlight the extent of this biological influence.  $\Delta$  NOx increased from spring (mean surface:  $3.13 \pm 1.64 \,\mu\text{M}$ ; mean deep:  $2.66 \pm 2.26 \,\mu\text{M}$ ) to summer (mean surface:  $5.76 \pm 1.99 \,\mu\text{M}$ ; mean deep:  $7.03 \pm 0.75 \,\mu\text{M}$ ). A similar trend was observed for  $\Delta$ Phosphate, rising from spring (mean surface:  $0.25 \pm 0.10 \,\mu\text{M}$ ; mean deep:  $0.20 \pm 0.10 \,\mu\text{M}$ ) to summer (mean surface:  $0.48 \pm 0.11 \,\mu\text{M}$ ; mean deep:  $0.48 \pm$ 0.04  $\mu$ M).  $\Delta$ Silicate also increased between seasons, from spring mean (surface: 1.65  $\pm$  0.66  $\mu$ M; mean deep:  $1.27 \pm 0.77 \mu$ M) to summer (mean surface:  $2.14 \pm 0.99 \mu$ M; mean deep: 3.28 $\pm$  0.25  $\mu$ M). These consistently larger summer  $\Delta$ Nutrient values strongly indicate enhanced biological uptake during the stratified summer, representing the cumulative effect of nutrient consumption that occurred since the spring bloom. In spring, slightly higher surface ΔNutrient values imply active phytoplankton uptake in the surface layer, potentially supported by vertical nutrient replenishment from underlying waters. During summer, the increase in  $\Delta NOx$  and  $\Delta Silicate$  at depth relative to the surface points to pronounced nutrient depletion in surface waters and subsequent export of organic matter. These elevated values at depth likely stem from sustained biological uptake beneath the surface or downward transport of nutrient-depleted waters, with limited remineralization en route, resulting in deep nutrient concentrations lower than predicted by conservative mixing. The modestly higher  $\Delta Phosphate$  at the surface may reflect suppressed phosphate uptake under nitrogen or silicate limitation, or additional phosphate input from glacial meltwater insufficiently captured in the PSWw end-member (Hawkings et al., 2016). Seasonal variability in phytoplankton activity was further examined through the relationship between chlorophyll-a and \( \Delta \) Nutrient (Fig. 6). In spring, the absence of significant correlations



302

303

304

305

306

307

308

309

310

311

312

313

314

315

316

317

318

319

320

321

322



(r<sup>2</sup> < 0.04) suggests that sampling preceded the main phytoplankton bloom, as supported by elevated background nutrient levels. In contrast, summer data revealed weak but significant negative correlations most notably for nitrate ( $r^2 = 0.15$ , p < 0.05) (Fig. 6d) and silicate ( $r^2 = 0.15$ , p < 0.05) 0.39, p < 0.01) (Fig. 6f), indicative of biological drawdown, particularly by diatoms. These observations are consistent with post-bloom conditions (Egge & Aksnes, 1992; Hodal et al., 2012) and align with the seasonal rise in surface N/P ratios (from 14.99 to 18.80), suggestive of NOx depletion following diatom-dominated productivity (Leu et al., 2011). The relationship between salinity and  $\Delta$ Nutrient exhibited clear seasonal contrasts (Fig. 7). In spring, all ΔNutrient values showed weak negative correlations with salinity—for instance,  $\Delta$ Phosphate ( $r^2 = 0.14$ ) (Fig. 7b) suggesting a reduced influence of high-salinity, nutrient-rich AW and MAW on biological drawdown. During summer, NOx ( $r^2 = 0.29$ ) (Fig. 7d) and phosphate ( $r^2 = 0.43$ ) (Fig. 7e) continued to show positive correlations, though NOx remained weak. By contrast, silicate was inversely related to salinity ( $r^2 = 0.94$ ) (Fig. 7f), suggesting an additional input from glacial meltwater associated with PSWw. This influx may obscure the biological drawdown signal typically expected for silicate. The weak summer correlation between  $\Delta$ Nutrient and chlorophyll-a is a critical finding, as it implies a temporal decoupling between cumulative nutrient consumption and instantaneous phytoplankton biomass. The consistently high ΔNutrient values observed in summer serve as a 'biogeochemical memory', reflecting the legacy of intense nutrient uptake during the preceding spring bloom. In contrast, the lower and more variable chlorophyll-a concentrations likely represent a snapshot of a post-bloom community, where phytoplankton biomass has been diminished by factors such as grazing and sinking. Therefore, this study demonstrates that





ΔNutrient is not merely a proxy for concurrent biological activity but rather a powerful integrated indicator that quantifies the total impact of seasonal biological processes on the nutrient inventory.

Interpretation of  $\Delta Silicate$  warrants particular attention, given the influence of non-conservative silicate input from glacial meltwater, which was not included as a separate end-member in our model. The strong negative correlation between observed silicate and salinity in summer ( $r^2 = 0.94$ , Fig. 7f) supports the presence of glacially sourced silicate (Hawkings et al., 2017). As a result, the calculated  $\Delta Silicate$  values likely underestimate the true biological drawdown. Therefore, the values presented here should be considered a conservative estimate of silicate consumption. Despite this limitation, elevated  $\Delta Silicate$  values during summer indicate that diatom-driven uptake was substantial, drawing down not only the silicate initially present in water masses but also the ongoing input from meltwater. Ambient concentrations approached potential limitation levels ( $\sim 2~\mu M$ ), underscoring the scale of biological consumption. Together, the underestimated yet high  $\Delta Silicate$  and the approach toward limiting concentrations provide strong evidence that biological processes, rather than physical mixing alone, regulate silicate dynamics in Kongsfjorden during the summer season.

#### 3.4. Seasonal Shift in Nutrient Limitation Patterns

The potential for nutrient limitations on phytoplankton growth in Kongsfjorden was evaluated using the N/P ratio and the absolute concentrations of key nutrients (Fig. 8; see also Section 3.1). During spring, the mean surface N/P ratio was  $15.0 \pm 2.7$ , while that in the mean deep-water was  $13.8 \pm 2.1$ . These values were slightly below or close to the canonical Redfield ratio of 16:1, suggesting that phytoplankton growth was not strongly limited by either nitrogen





345 or phosphorus during this period. If any trend was present, it may have leaned toward mild 346 nitrogen limitation. The relatively uniform N/P ratios with increasing depth also indicated 347 effective vertical mixing in spring. 348 In contrast, the summer season exhibited a pronounced increase in the surface N/P ratio, 349 averaging  $18.8 \pm 7.0$  and exceeding the Redfield ratio. This shift strongly suggests a transition 350 toward phosphorus limitation in surface waters. The deep-layer N/P ratio remained lower 351 (mean:  $13.2 \pm 3.8$ ), resulting in a marked vertical divergence. This contrast emphasizes the role of enhanced summer stratification in establishing distinct biogeochemical regimes in the 352 surface and deep layers. 353 The possibility of phosphorus limitation in summer surface waters was supported by the 354 355 absolute phosphate concentrations observed during this period. The mean summer surface 356 phosphate concentration (0.13  $\pm$  0.07  $\mu$ M) fell below the commonly used 0.2  $\mu$ M threshold indicating phosphorus limitation for Arctic phytoplankton (Tremblay et al., 2015). 357 Concurrently, the mean surface silicate concentration during summer was  $1.66 \pm 0.39 \mu M$ , 358 approaching the 2 µM threshold commonly associated with potential silicate limitation for 359 360 diatom growth (Egge & Aksnes, 1992). This nutrient regime, characterized by low phosphate ( $< 0.2 \mu M$ ) and low silicate ( $< 2 \mu M$ ), likely imposed significant selective pressure on the 361 phytoplankton community, potentially favoring the dominance of small flagellates, which are 362 more competitive under nutrient-depleted conditions, particularly phosphorus limitation, over 363 diatoms (Degerlund & Eilertsen, 2010; Larsen et al., 2004; Egge & Aksnes, 1992). 364 These observed seasonal shifts in nutrient limitation patterns were closely linked to 365 366 phytoplankton community succession. In Arctic waters, spring diatom blooms typically deplete





large amounts of NOx and silicate. Following these blooms, summer conditions, which are marked by stratification and altered nutrient ratios, may favor the dominance of other phytoplankton groups, including nitrogen-fixing microalgae or small species with distinct nutrient uptake strategies (Leu et al., 2011; Sakshaug, 2004). The observed increase in the surface N/P ratio from spring to summer supports this interpretation, as it indicates a faster depletion of phosphate relative to NOx following the spring diatom bloom. This pattern is consistent with the known consequences of intense spring diatom blooms in Arctic fjords. While these blooms consume large amounts of NOx and silicate, the post-bloom summer conditions, characterized by stratified and nutrient-depleted surface waters, often lead to a shift toward phosphorus limitation, as observed in our study. This succession favors smaller phytoplankton with distinct uptake strategies (Hodal et al., 2012; Leu et al., 2011).

# 4. Conclusion

The present study highlighted significant seasonal differences in water mass mixing and nutrient dynamics in Kongsfjorden, Svalbard. Spring conditions were dominated by MAW and active vertical mixing, resulting in relatively high and uniform nutrient concentrations, with N/P ratios near the Redfield ratio, suggesting nutrient-replete conditions. In contrast, summer featured increased surface freshening from PSW and PSW<sub>W</sub> due to meltwater input, leading to strong stratification. This physical structure, together with enhanced biological uptake reflected by large ΔNutrient values, led to substantial reductions in observed surface concentrations of NOx (~69%), phosphate (~74%), and silicate (~47%) compared to spring. The ΔNutrient metric effectively captured the cumulative biological drawdown over the season, acting as a 'biogeochemical memory' that is decoupled from instantaneous biomass. As a result, summer

https://doi.org/10.5194/egusphere-2025-2845 Preprint. Discussion started: 27 June 2025 © Author(s) 2025. CC BY 4.0 License.





surface waters shifted toward the potential co-limitation of phosphorus (N/P  $\sim$ 18.8; phosphate  $\sim$ 0.13  $\pm$  0.07  $\mu$ M) and silicate ( $\sim$ 1.66  $\pm$  0.39  $\mu$ M). These results suggest a seasonal transition from a well-mixed, nutrient-rich spring regime to a stratified, nutrient-limited summer system driven by biological processes. Understanding these dynamics is essential for predicting how Arctic fjord ecosystems may respond to ongoing climate change, which is expected to affect the water mass structure, meltwater input, and stratification, thus altering nutrient cycling and primary productivity.

https://doi.org/10.5194/egusphere-2025-2845 Preprint. Discussion started: 27 June 2025 © Author(s) 2025. CC BY 4.0 License.





# **Author contributions**

HK wrote the original draft and performed visualization and formal analysis. THK was involved in the review and editing of the manuscript, funding acquisition, and conceptualization. DH contributed to the review and editing of the manuscript and conducted the investigation. SRP contributed to the review and editing of the manuscript and provided critical input for the conceptualization of the study.

https://doi.org/10.5194/egusphere-2025-2845 Preprint. Discussion started: 27 June 2025 © Author(s) 2025. CC BY 4.0 License.





# Acknowledgments

We would like to thank all MBL members for their support with the sample analysis. This study was supported by Korea Institute of Marine Science and Technology Promotion (KIMST) funded to the Ministry of Oceans and Fisheries, Korea (RS-2025-02304432) and by the Korea Institute of Ocean Science and Technology (PEA0330).

408





409	References							
410	Arrigo, K. R., Perovich, D. K., Pickart, R. S., Brown, Z. W., van Dijken, G. L., Lowry, K.							
411	E., Mills, M. M., Palmer, M. A., Balch, W. M., Bates, N. R., Benitez-Nelson, C. R.,							
412	Brownlee, E., Frey, K. E., Laney, S. R., Mathis, J., Matsuoka, A., Greg Mitchell, B., Moore,							
413	G. W. K., Reynolds, R. A., Sosik, H. M., and Swift, J. H.: Phytoplankton blooms beneath							
414	the sea ice in the Chukchi sea, Deep Sea Research Part II: Topical Studies in Oceanography,							
415	105, 1–16, https://doi.org/10.1016/j.dsr2.2014.03.018, 2014.							
416	Carmack, E. and Wassmann, P.: Food webs and physical-biological coupling on pan-							
417	Arctic shelves: Unifying concepts and comprehensive perspectives, Progress in							
418	Oceanography, 71, 446–477, https://doi.org/10.1016/j.pocean.2006.10.004, 2006.							
419	Codispoti, L. A., Kelly, V., Thessen, A., Matrai, P., Suttles, S., Hill, V., Steele, M., and							
420	Light, B.: Synthesis of primary production in the Arctic Ocean: III. Nitrate and phosphate							
421	based estimates of net community production, Progress in Oceanography, 110, 126-150,							
422	https://doi.org/10.1016/j.pocean.2012.11.006, 2013.							
423	Degerlund, M. and Eilertsen, H. C.: Main Species Characteristics of Phytoplankton Spring							
424	Blooms in NE Atlantic and Arctic Waters (68–80° N), Estuaries and Coasts, 33, 242–269,							
425	https://doi.org/10.1007/s12237-009-9167-7, 2010.							
426	Duarte, C. M., Lenton, T. M., Wadhams, P., & Wassmann, P. (2012). Abrupt climate							
427	change in the Arctic. Nature Climate Change, 2(2), 60-62. doi:10.1038/nclimate1386							
428	Duarte, P., Meyer, A., and Moreau, S.: Nutrients in Water Masses in the Atlantic Sector of							
429	the Arctic Ocean: Temporal Trends, Mixing and Links With Primary Production, Journal							
430	of Geophysical Research: Oceans, 126, e2021JC017413,							





431 https://doi.org/10.1029/2021JC017413, 2021. Egge, J. K., & Aksnes, D. L. (1992). Silicate as regulating nutrient in phytoplankton 432 competition. Marine Ecology Progress Series, 83, 281–289. 433 434 Falk-Petersen, S., Haug, T., Hop, H., Nilssen, K. T., and Wold, A.: Transfer of lipids from plankton to blubber of harp and hooded seals off East Greenland, Deep Sea Research Part 435 II: **Topical** Studies 56, 2080-2086, 436 in Oceanography, https://doi.org/10.1016/j.dsr2.2008.11.020, 2009. 437 Galloway, J. N., Dentener, F. J., Capone, D. G., Boyer, E. W., Howarth, R. W., Seitzinger, 438 S. P., Asner, G. P., Cleveland, C. C., Green, P. A., Holland, E. A., Karl, D. M., Michaels, 439 A. F., Porter, J. H., Townsend, A. R., and Vöosmarty, C. J.: Nitrogen Cycles: Past, Present, 440 and Future, Biogeochemistry, 70, 153-226, https://doi.org/10.1007/s10533-004-0370-0, 441 2004. 442 Gradinger, R.: Climate change and biological oceanography of the Arctic Ocean, 443 Philosophical Transactions of the Royal Society of London. Series A: Physical and 444 Engineering Sciences, 352, 277–286, https://doi.org/10.1098/rsta.1995.0070, 1997. 445 446 Hegseth, E. N. and Tverberg, V.: Effect of Atlantic water inflow on timing of the 447 phytoplankton spring bloom in a high Arctic fjord (Kongsfjorden, Svalbard), Journal of Marine Systems, 113–114, 94–105, https://doi.org/10.1016/j.jmarsys.2013.01.003, 2013. 448 449 Hodal, H., Falk-Petersen, S., Hop, H., Kristiansen, S., and Reigstad, M.: Spring bloom dynamics in Kongsfjorden, Svalbard: nutrients, phytoplankton, protozoans and primary 450 production, Polar Biol, 35, 191–203, https://doi.org/10.1007/s00300-011-1053-7, 2012. 451 452 Holmes, R. M., McClelland, J. W., Peterson, B. J., Shiklomanov, I. A., Shiklomanov, A.





453 I., Zhulidov, A. V., Gordeev, V. V., and Bobrovitskaya, N. N.: A circumpolar perspective 454 on fluvial sediment flux to the Arctic ocean, Global Biogeochemical Cycles, 16, 45-1-45-455 14, https://doi.org/10.1029/2001GB001849, 2002. Larsen, A., Flaten, G. A. F., Sandaa, R.-A., Castberg, T., Thyrhaug, R., Erga, S. R., Jacquet, 456 S., and Bratbak, G.: Spring phytoplankton bloom dynamics in Norwegian coastal waters: 457 Microbial community succession and diversity, Limnology and Oceanography, 49, 180-458 190, https://doi.org/10.4319/lo.2004.49.1.0180, 2004. 459 460 Leu, E., Wiktor, J., Søreide, J. E., Berge, J., and Falk-Petersen, S.: Increased irradiance reduces food quality of sea ice algae, Marine Ecology Progress Series, 411, 49-60, 461 462 https://doi.org/10.3354/meps08647, 2010. Miller, Arthur R.. 1950. "A study of mixing processes over the edge of the continental 463 shelf." Journal of Marine Research 9, (2). 464 Nilsen, F., Cottier, F., Skogseth, R., and Mattsson, S.: Fjord-shelf exchanges controlled by 465 ice and brine production: The interannual variation of Atlantic Water in Isfjorden, Svalbard, 466 Continental Shelf Research, 28, 1838–1853, https://doi.org/10.1016/j.csr.2008.04.015, 467 468 2008. Polyakov, I. V., Pnyushkov, A. V., and Timokhov, L. A.: Warming of the Intermediate 469 Atlantic Water of the Arctic Ocean in the 2000s, https://doi.org/10.1175/JCLI-D-12-470 00266.1, 2012. 471 472 Randelhoff, A., Holding, J., Janout, M., Sejr, M. K., Babin, M., Tremblay, J.-É., and Alkire, M. B.: Pan-Arctic Ocean Primary Production Constrained by Turbulent Nitrate Fluxes, 473 474 Front. Mar. Sci., 7, https://doi.org/10.3389/fmars.2020.00150, 2020.





475 Reigstad, M., Wexels Riser, C., Wassmann, P., and Ratkova, T.: Vertical export of 476 particulate organic carbon: Attenuation, composition and loss rates in the northern Barents 477 Sea, Deep Sea Research Part II: Topical Studies in Oceanography, 55, 2308-2319, https://doi.org/10.1016/j.dsr2.2008.05.007, 2008. 478 479 Rudels, B., Meyer, R., Fahrbach, E., Ivanov, V. V., Østerhus, S., Quadfasel, D., Schauer, U., Tverberg, V., and Woodgate, R. A.: Water mass distribution in Fram Strait and over 480 the Yermak Plateau in summer 1997, Annales Geophysicae, 18, 687-705, 481 482 https://doi.org/10.1007/s00585-000-0687-5, 2000. 483 Rudels, B., Björk, G., Nilsson, J., Winsor, P., Lake, I., and Nohr, C.: The interaction 484 between waters from the Arctic Ocean and the Nordic Seas north of Fram Strait and along 485 the East Greenland Current: results from the Arctic Ocean-02 Oden expedition, Journal of Marine Systems, 55, 1–30, https://doi.org/10.1016/j.jmarsys.2004.06.008, 2005. 486 487 Rysgaard, S., Nielsen, T. G., and Hansen, B. W.: Seasonal variation in nutrients, pelagic primary production and grazing in a high-Arctic coastal marine ecosystem, Young Sound, 488 489 Northeast Greenland, Marine **Ecology Progress** Series, 179, 13-25, https://doi.org/10.3354/meps179013, 1999. 490 Sakshaug, E.: Primary and Secondary Production in the Arctic Seas, in: The Organic 491 492 Carbon Cycle in the Arctic Ocean, edited by: Stein, R. and MacDonald, R. W., Springer, 493 Berlin, Heidelberg, 57–81, https://doi.org/10.1007/978-3-642-18912-8\_3, 2004. Singh, A., David T., D., Tripathy, S. C., and Naik, R. K.: Interplay of regional 494 oceanography and biogeochemistry on phytoplankton bloom development in an Arctic 495 106916, 496 fjord, Estuarine, Coastal and Shelf Science, 243,



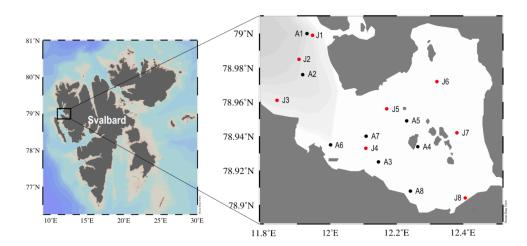


497	https://doi.org/10.1016/j.ecss.2020.106916, 2020.
498	Torres-Valdés, S., Tsubouchi, T., Bacon, S., Naveira-Garabato, A. C., Sanders, R.,
499	McLaughlin, F. A., Petrie, B., Kattner, G., Azetsu-Scott, K., and Whitledge, T. E.: Export
500	of nutrients from the Arctic Ocean, Journal of Geophysical Research: Oceans, 118, 1625-
501	1644, https://doi.org/10.1002/jgrc.20063, 2013.
502	Tremblay, JÉ., Anderson, L. G., Matrai, P., Coupel, P., Bélanger, S., Michel, C., and
503	Reigstad, M.: Global and regional drivers of nutrient supply, primary production and CO2
504	drawdown in the changing Arctic Ocean, Progress in Oceanography, 139, 171-196,
505	https://doi.org/10.1016/j.pocean.2015.08.009, 2015.
506	Tomczak, Matthias. 1999. "Some historical, theoretical and applied aspects of quantitative
507	water mass analysis." Journal of Marine Research 57, (2).
508	Tovar-Sánchez, A., Duarte, C. M., Alonso, J. C., Lacorte, S., Tauler, R., and Galbán-
509	Malagón, C.: Impacts of metals and nutrients released from melting multiyear Arctic sea
510	ice, Journal of Geophysical Research: Oceans, 115, https://doi.org/10.1029/2009JC005685,
511	2010.
512	Vonnahme, T. R., Klausen, L., Bank, R. M., Michellod, D., Lavik, G., Dietrich, U., and
513	Gradinger, R.: Light and freshwater discharge drive the biogeochemistry and microbial
514	ecology in a sub-Arctic fjord over the Polar night, Front. Mar. Sci., 9,
515	https://doi.org/10.3389/fmars.2022.915192, 2022.
516	Wassmann, P.: Arctic marine ecosystems in an era of rapid climate change, Progress in
517	Oceanography, 90, 1–17, https://doi.org/10.1016/j.pocean.2011.02.002, 2011.





Figure 1. Map of the study area in Kongsfjorden, which is located on the west coast of
Spitsbergen, Svalbard. Sampling stations from the spring (April 2023) and summer (July 2023)
cruises are shown. Black circles represent spring and red circles represent summer.



522





**Figure 2.** (a) Temperature–salinity (T–S) diagram showing the four end-member water types used in this study: Atlantic Water (AW), Modified Atlantic Water (MAW), Polar Surface Water (PSW), and warm Polar Surface Water (PSWw). These end-members were defined based on previously published criteria (e.g., Rudels et al., 2000) and supported by hydrographic data collected during the cruises (Table 1). (b) Conceptual diagram of the four-end-member mixing framework. Point P denotes an arbitrary water parcel in T–S space. Its location relative to the end-members was used to estimate fractional contributions ( $f_A$ ,  $f_B$ ,  $f_C$ , and  $f_D$ ), with the sum constrained to unity ( $f_A + f_B + f_C + f_D = 1$ ).

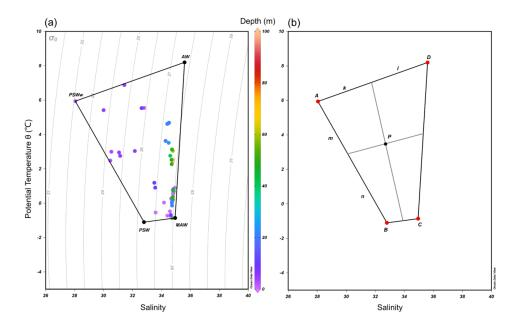






**Figure 3.** Vertical profiles of (a) temperature (°C), (b) salinity, and (c) nitrate ( $\mu$ M), (d) phosphate ( $\mu$ M), and (e) silicate levels ( $\mu$ M) in Kongsfjorden. Black circles indicate spring data; red circles indicate summer data. Data represent measurements from multiple stations and depths.

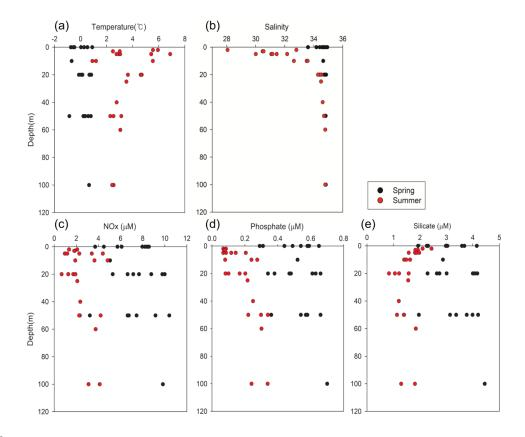
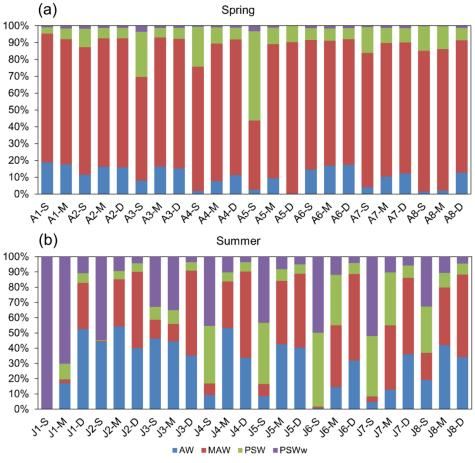






**Figure 4.** Relative contributions of the four end-member water masses (AW, MAW, PSW, and PSWw) in Kongsfjorden during (a) spring and (b) summer based on the four-component mixing model. Labels on the x-axis indicate the sampling station followed by the relative sampling depth: S (Surface), M (Mid-depth), and D (Deep). For the spring cruise (a), S, M, and D samples were typically collected at 0 m, 20 m, and 50 m, respectively (except for station A2, where D was 100 m). For the summer cruise (b), sampling depths varied by station, with S samples from 0-5 m, M from 10-25 m, and D from 50-100 m for all stations except J1. At station J1, S, M, and D samples were collected at 2 m, 5 m, and 20 m, respectively.



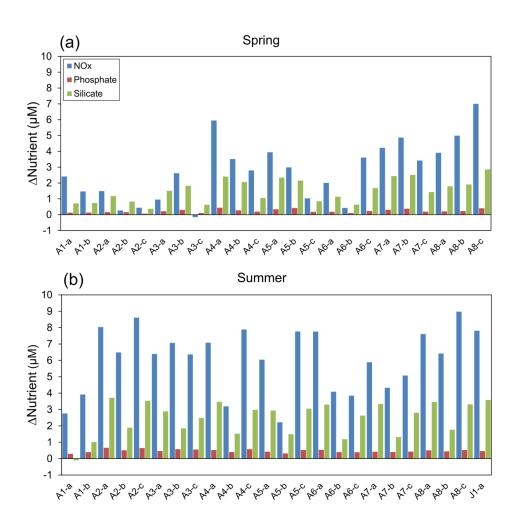


549

550



Figure 5. Differences between theoretical (mixing-derived) and observed nutrient concentrations ( $\Delta$ Nutrient = Theoretical – Observed;  $\mu$ M) during (a) spring and (b) summer. Bars represent  $\Delta$ Nutrient values for nitrate, phosphate, and silicate, as indicated in the legend.



551





Figure 6. Relationships between chlorophyll-a (mg/m³) and ΔNutrient (μM) in Kongsfjorden: (a–c) spring, (d–f) summer. Regression lines and r² values are shown for each panel.

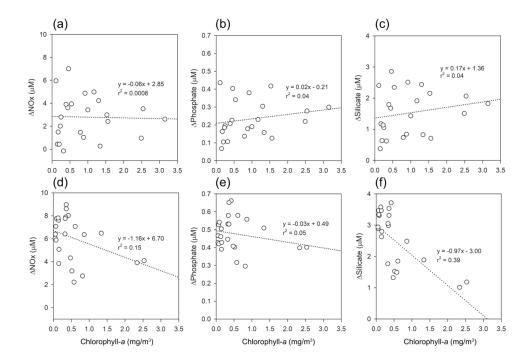
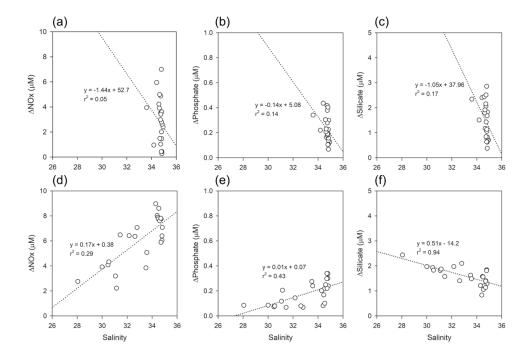






Figure 7. Relationships between salinity and ΔNutrient (μM) in Kongsfjorden: (a–c) spring,

558 (d-f) summer. Regression lines and r<sup>2</sup> values are shown for each panel.







- Figure 8. Vertical profiles of the nitrogen-to-phosphorus (N/P) molar ratio in Kongsfjorden.
- White circles represent spring values; black circles represent summer. The vertical dashed line
- indicates the Redfield ratio (16:1).

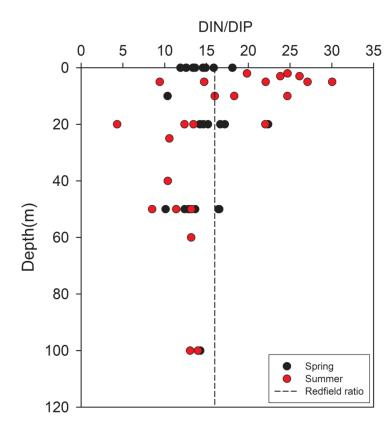






**Table 1.** Temperature ( ${}^{\circ}$ C), salinity, and nutrient concentrations (nitrate, phosphate, and silicate;  $\mu$ M) for the four end-member water types: Atlantic Water (AW), Modified Atlantic Water (MAW), Polar Surface Water (PSW), and warm Polar Surface Water (PSWw). The temperature-salinity (T-S) definitions were adopted from Rudels et al. (2000), with  $\sigma_0$  represents the potential density anomaly referenced to 0 dbar. determined based on the characteristics of the most representative samples collected in this study (identified at the vertices of the T-S diagram in Fig. 2a). Nutrient values for each water mass are based on literature values from Duarte et al. (2021).

End member	Water mass	NOx (μM)	Phosphate (µM)	Silicate (µM)	Temperature (°C)	Salinity	Reference (Rudels et al. 2000)
A	Atlantic Water (AW)	10.66	0.82	4.86	8.2	35.6	$27.70 < \sigma_0 < 27.97, T >$ $2^{\circ}\text{C, or } 27.97 < \sigma_0,$ and $\sigma_{0.5} < 30.444, T > 0^{\circ}\text{C}$
В	Modified Atlantic Water (MAW)	10.55	0.78	4.94	-0.86	34.95	$\begin{array}{l} 27.70 < \sigma_0 < 27.97, T < 0^{\circ}\text{C}, \\ \text{S} < 34.676 + 0.232 \cdot \\ \text{T, or } 27.97 < \sigma_0, \ and \ \sigma_{0.5} < \\ 30.444, \ T > 0^{\circ}\text{C} \end{array}$
С	Polar Surface water (PSW)	6.91	0.56	3.85	-1.1	32.8	$27.70 > \sigma_0, T < 0$ °C
D	Polar Surface water warm (PSWw)	4.83	0.38	2.33	5.94	28.05	$27.70 > \sigma_0, \ T > 0 ^{\circ}\text{C}$